Sustinere
Journal of Environment and Sustainability
Volume 6 Number 2 (2022) 92-101

Print ISSN: 2549-1245 Online ISSN: 2549-1253
Website: https://sustinerejes.com E-mail: sustinere.jes@iain-surakarta.ac.id

RESEARCH PAPER

Spatio-temporal analysis of built-up area and land surface temperature in Surakarta using Landsat imageries

Vidya Nahdhiyatul Fikriyah*, Danardono, M. Iqbal Taufiqurrahman Sunariya, Munawar Cholil, Tegar Abdul Hafid, Muhammad Ismail Islam

Faculty of Geography, Universitas Muhammadiyah Surakarta, Kartasura, Sukoharjo, Central Java, Indonesia 57162

Article history:
Received 23 April 2021 | Accepted 1 April 2022 | Available online 31 August 2022

Abstract. The need for built-up areas continues to increase, along with the increasing population in the city of Surakarta and its surrounding. This condition affects the land surface temperature which then leads to the change in climatic conditions. The availability of land for settlement and surface temperature will affect the comfort level of living in a city. For this reason, this study aims to map the distribution of built-up area and the surface temperature of Surakarta city and discusses the relationship between these two aspects spatially and temporally. The data used are Landsat imageries recorded in 2000, 2013, and 2019. The built-up area was identified using Normalized Difference Built-Up Index (NDBI), while the temperature data was obtained through thermal band processing using Land Surface Temperature (LST) method. The results showed that during the period of the study, the built-up area and the surface temperature in Surakarta and its surroundings increased, especially in the eastern and southern parts of Surakarta. The results also showed that there is a positive correlation between the built-up index and its surface temperature.

Keywords: built-up area; NDBI; LST; Landsat; Surakarta

1. Introduction

Surakarta is a city that has experienced a rapid population growth. According to Statistics Indonesia or BPS (2020), the total population of Surakarta City was 519,587 in 2019, while the total population in 2000 and 2013 was recorded only 490,214 and 507,825, respectively.

This rise in population will certainly be followed by the increase in the demand for (built-up) areas either for dwelling or working, which in turn will reduce the existence of green open spaces (Putri & Zain, 2010). This development of built-up area then affects the quality of the residential environment, due to the existence of denser buildings (Yuliastuti et al., 2012; Imran et al., 2021). Moreover, the increase of concentration in these buildings has also led to the emergence of the UHI (Urban Heat Island) phenomenon in urban areas (Guha et al., 2018; Rushayati et al., 2018). In summary, the conversion of land cover/use from non-built-up to the built-up area will eventually affect the temperature around Surakarta, resulting in a reduced level of comfort to live.

*Corresponding author. E-mail: vnf684@ums.ac.id
DOI: https://doi.org/10.22515/sustinere.jes.v6i2.187

Surface temperature affects not only the comfort conditions but also other aspects of the urban environment, such as rainfall (Adeanti & Harist, 2018). In addition, the surface temperature is also an important parameter to explain the physical conditions of the environment and climate models including the energy balance both locally and globally (Malik et al., 2019; Hidayati & Suharyadi, 2019; Danardono et al., 2021). In consequence, surface temperature monitoring is an important activity to do as an effort to identify changes in the environment (Macarof et al., 2017), especially if these changes occur in urban areas where the anthropogenic activities are high (Srivanit & Hokao, 2009; Hadibasyir et al., 2020). Because the land cover/land use conditions in urban areas are heterogeneous resulting in dynamics in surface temperature, which both are seen in its spatial and temporal distribution.

Regarding the technique in the observation of biophysical conditions, the development of remote sensing technology has made possible the identification of built-up area and surface temperature for a large study area (regionally and globally) to be more effective in comparison to the direct field measurement (Srivanit & Hokao, 2009). Remote sensing can provide an overview of the condition of the earth's surface on satellite images repeatedly, enabling monitoring and identification of changes in land cover/use (Deng et al., 2019; Kabisch et al., 2019). In addition, remote sensing data can also display the variations in the appearance of the earth's surface, coming from variations in image specifications, including spatial and temporal resolution (Kalma et al., 2008). Specifically, the use of thermal channels in Landsat imageries can extract data on the earth's surface temperature (Wiweka, 2014).

As the dynamic characteristic of built-up and surface temperature on earth, therefore, it is necessary to measure the built-up land and surface temperature in the study area which is reviewed spatially and temporally. For that reason, the objectives of the present study are to map the distribution of built-up area and surface temperature of Surakarta city and to analyze the relationship between these two aspects, both from the spatial distribution and the time difference. Observations were made based on remote sensing data over a long period of time. The results of this analysis are expected to be able to provide up-to-date information regarding the condition of built-up area distribution and temperature in Surakarta. Hence, it can become a reference for the evaluation of urban spatial planning in the future.

2. Research Methods

2.1. Study area

The study area is the city of Surakarta (Figure 1), which is located geographically between 110°45'15"- 110°45'35" East Longitude and 7°36'00"- 7°56'00" South Latitude. The location of Surakarta City is also bordered by three other districts/regencies, namely Karanganyar, Sukoharjo, and Boyolali.

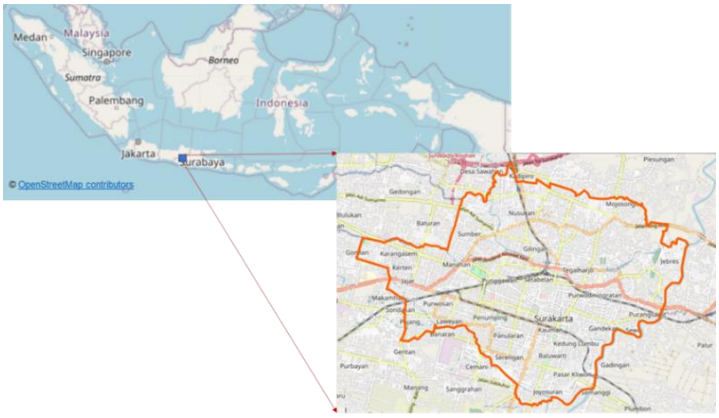

Figure 1. Location of Surakarta City as study area (www.openstreetmap.org).

The city has an area of 44.04 km^2 where the total area is divided into five sub-districts which can be seen in detail in Table 1. The most densely populated sub-district is Pasar Kliwon (16,033.20 people/km^2), while Laweyan is the sub-district with the lowest population density having 10,364.24 people/km^2 (BPS, 2020).

Table 1. Surakarta's area, population, and population density by sub-district in 2019.

District	Area (km^2)	Percentage %	Population (thousand)	Population density (per km^2)
Laweyan	8.64	19.62	89,547	10,364.24
Serengan	3.19	7.24	45,424	14,239.50
Pasar Kliwon	4.82	10.95	77,280	16,033.20
Jebres	12.58	28.56	143,650	11,418.92
Banjarsari	14.81	33.63	163,686	11,052.40

Source: BPS (2020)

2.2. Data processing and methods

The process of collecting, processing, and analyzing data was carried out in several stages starting from image correction, the transformation of the Normalized Difference Built-up Index (NDBI) and Land Surface Temperature (LST) to the regression analysis, as indicated on the following flow chart (Figure 2).

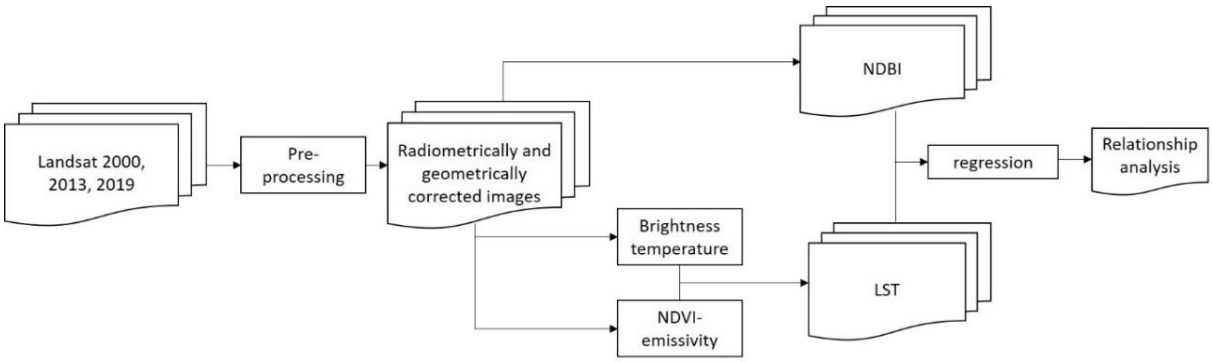

Figure 2. Flow chart of data processing and analysis of the present study.

The following is a full explanation for each stage:

a. Image preparation

This study used 2 types of Landsat imagery, namely Landsat 7 ETM + (Enhanced Thematic Mapper +) for the 2000 recording and Landsat 8 OLI-TIRS (Operational Land Imager-Thermal Infrared Sensor) imagery for the image recorded in 2013 and 2019. Considering the slow pace of development in the built-up area, the observation was carried out for almost 20 years (observation was done once every 10 years). This was done to see more visible changes in the built-up area. Furthermore, in order to use the latest version of Landsat imagery, the year 2013 was chosen because Landsat 8 was launched in that year.

To fulfil the aims of the study, three images were needed and acquired freely at level 1 from the website of Earth Explorer (https://earthexplorer.usgs.gov). The downloaded thermal bands of Landsat have been resampled in resolution to 30m (USGS, 2018) to match with the resolution of multispectral bands. The thermal bands were then corrected to the sensor radiance (for band 6 in Landsat 7 and band 10 in Landsat 8). The correction was also performed for the visible and infrared bands (near-infrared and shortwave infrared) to extract the surface reflectance using the

Dark Object Subtraction (DOS) method (specifically for bands 3, 4, 5 in Landsat 7 and bands 4, 5, 6 in Landsat 8).

Figure 3 shows Landsat imagery for the three years of observation, which is displayed with a pseudo-colour composite combining near-infrared, red, and green bands, while Table 2 presents a detailed specification of the images used.

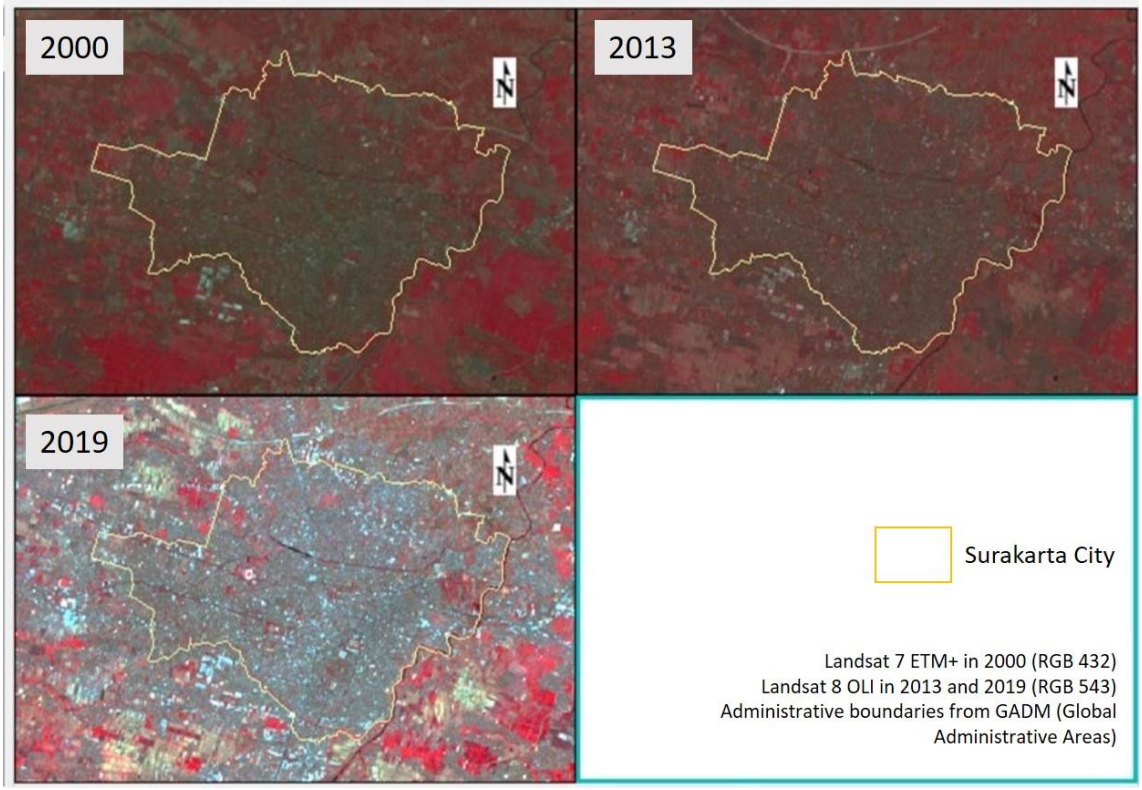

Figure 3. Landsat imageries for showing the condition of Surakarta City in 2000, 2013, and 2019.

Table 2. Specifications for Landsat imageries used in the study.

Image ID	Sensor	Time of acquisition	Path/ row	Spatial resolution
LE71190652000173SGS00	Landsat 7 ETM+	21-06-2000	119/65	30 m
LC81190652013248LGN01	Landsat 8 OLI- TIRS	05-09-2013	119/65	30 m
LC81190652019297LGN00	Landsat 8 OLI- TIRS	24-10-2019	119/65	30 m

b. Extraction of Normalized Difference Built-up Index (NDBI) data

The building density data was extracted from NDBI calculations that used the reflection of objects in the near-infrared (NIR) band, which are band 4 of Landsat 7 or band 5 of Landsat 8. The shortwave infrared bands refer to band 5 of Landsat 7 or band 6 of Landsat 8. The NDBI formula is as follows (Balew & Korme, 2020).

$$NDBI = \frac{SWIR - NIR}{SWIR + NIR} \quad (1)$$

c. Extraction of Land Surface Temperature (LST) data

The spectral radiance values in the thermal band (band 6 and 10 of Landsat 7 and 8, respectively) were then converted to Land Surface Temperature (LST). To obtain LST data, however, several steps were needed to be done in advance. The first was the calculation of the brightness temperature (Tb), and the second was the calculation of the Normalized Difference Vegetation Index (NDVI), and emissivity. Equation 2 was used to obtain the brightness temperature values (Xiong et al., 2012).

$$Tb = \frac{K2}{ln\frac{K1}{L\lambda} + 1} \quad (2)$$

where.

Tb= Brightness temperature (Kelvin)
K1= Band-specific thermal conversion constant from the metadata
K2= Band-specific thermal conversion constant from the metadata
L_{λ}= Top of Atmosphere spectral radiance (Watts/m^2.srad.μm)

The next step was the calculation of the Normalized Difference Vegetation Index (NDVI) using the near-infrared (NIR) and red band, in which Landsat 7 are band 4 and 3, respectively, while Landsat 8 are band 5 and 4. The NDVI formula is presented in the following equation (Balew & Korme, 2020).

$$NDVI = \frac{NIR - Red}{NIR + Red} \quad (3)$$

Afterward, the NDVI was used to calculate the emissivity value (ε) with the value classes shown in Table 3.

Table 3. Emissivity for each NDVI value (Zhang et al., 2006).

NDVI value	Emissivity value
< -0.18	0.985
-0.18 ≤ NDVI < 0.157	0.955
0.157 ≤ NDVI < 0.727	1.0094 + 0.047*Ln (NDVI)
≥ 0.727	0.990

The next step, from the brightness temperature and emissivity data, then the brightness temperature values can be generated through this equation (Kumari et al., 2018; Xiong et al., 2012).

$$\text{LST} = \frac{Tb}{1+\left(\lambda \times \frac{Tb}{\rho}\right)\ln \varepsilon} \quad (4)$$

Where,

LST = Land Surface Temperature (Kelvin)
Tb = Brightness temperature
λ = wavelength of emitted radiance (11.5 μm)
ρ = Planck constant multiplied by the velocity of light and divided by Boltzman constant (1.438×10^{-2} mk)
ε = land surface emissivity

d. Analysis of the relationship between NDBI and LST

The final stage was to perform a regression analysis comparing the NDBI and LST values. Regression was carried out for each observation year (2000, 2013, and 2019). This was done to produce equations that could explain the effect of NDBI values on LST. A number of 100 sample points were extracted randomly for regression between NDBI (as the independent variable) and LST (as the dependent variable). This regression produced an R-value which shows the degree of correlation between NDBI and LST, and R^2 value (coefficient of determination) which indicates how much the contribution of NDBI to LST.

3. Results and Discussion

3.1. Distribution of built-up area

The observation of built-up area distribution in the city of Surakarta was carried out based on the NDBI value from three years of image recording. The results of NDBI processing are shown in Figure 5, showing that there is a class value ranging from -0.8 to 0.5. In general, the range of NDBI values will be ranged from -1 to 1, where the NDBI value closer to 1 indicates a high building density condition, while a negative NDBI value means that the area is classified as a non-built-up area (Naserikia et al., 2019).

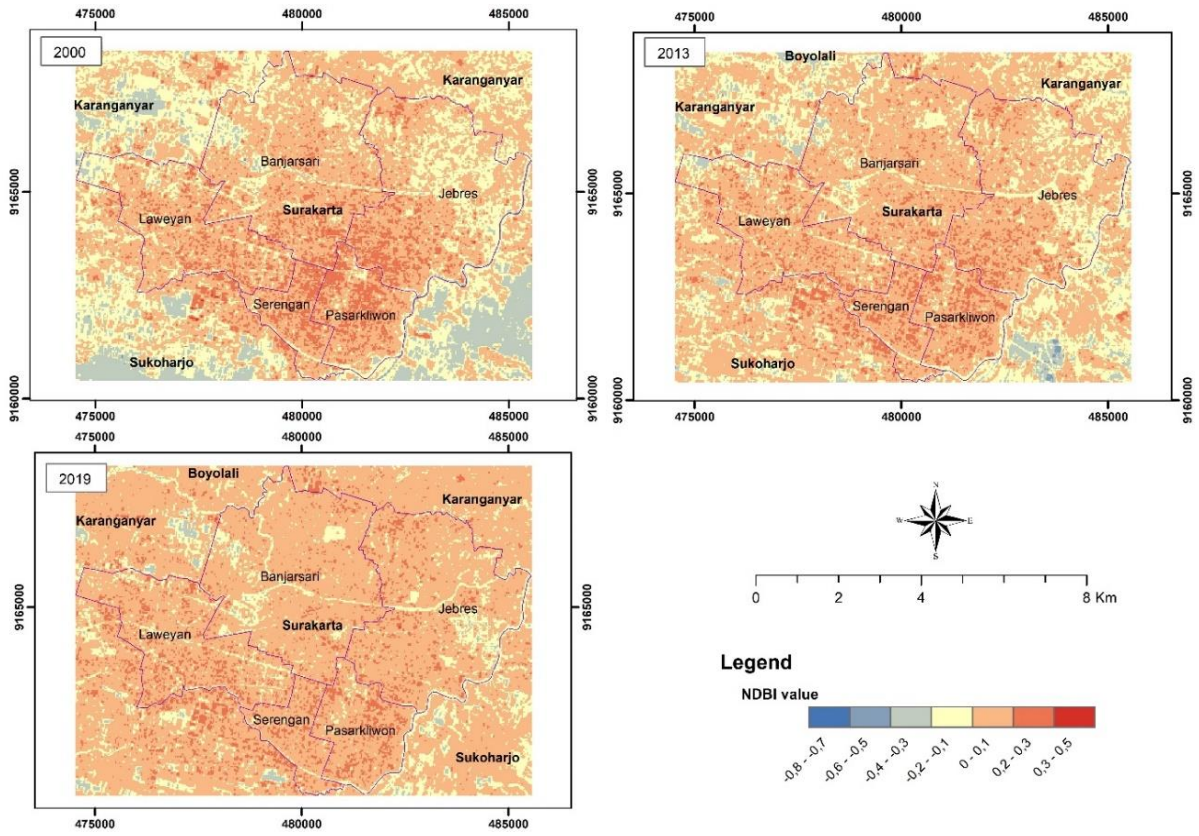

Figure 4. The distribution of NDBI values as an indicator of building density in Surakarta.

Based on Figure 4, it is known that in 2000, the southern and southeastern parts of Surakarta City show a densely built-up area. However, there are still many undeveloped areas on the north and northeast sides of Surakarta. Looking at the development 13 years later (in 2013), it appears that the built-up area is increasingly spreading to the north of the city. The phenomenon of built-up area spreading can also be observed in the surrounding districts of Surakarta, as seen in

Boyolali and Karanganyar (on the north side) and Sukoharjo (on the south side). The non-built-up area can still be seen in the northeastern part of the city of Surakarta, especially in Jebres and Banjarsari sub-districts. Furthermore, at the end of the observation year (2019), the built-up area has spread across almost all areas of Surakarta city and its surrounding districts. The conversion to the built-up area is evident especially in Sukoharjo on the southeast side of Surakarta City. This result strengthens the previous study stating that NDBI is sensitive to land conditions (in order to distinguish between built-up and open areas), which make it a common algorithm used as an index for the built-up area (Hidayati et al., 2017; Guha et al., 2018; Osgouei et al., 2019).

3.2. Land Surface temperature distribution

The land surface temperature conditions in Surakarta City at three different times are shown in Figure 5. Through visual observation, from Figure 5, it can be seen that in 2000 the City of Surakarta and its surroundings were dominated by classes of surface temperatures below 30^{0}C, especially on the northeast side of the city (Jebres District). This condition is in accordance with the density of buildings in Jebres Subdistrict, which is not too crowded this year (Figure 4).

Changes in surface temperature class occurred in the observation in 2013. In that year, the value of surface temperature was in the class between 30-39^{0}C, especially if seen from the southern side of Surakarta (sub-district of Serengan and Pasar Kliwon). A higher measured surface temperature up to the class of 43-45^{0}C was then observed in 2019. Areas with warmer temperatures especially were located in the east and south of the city of Surakarta and also in Sukoharjo Regency.

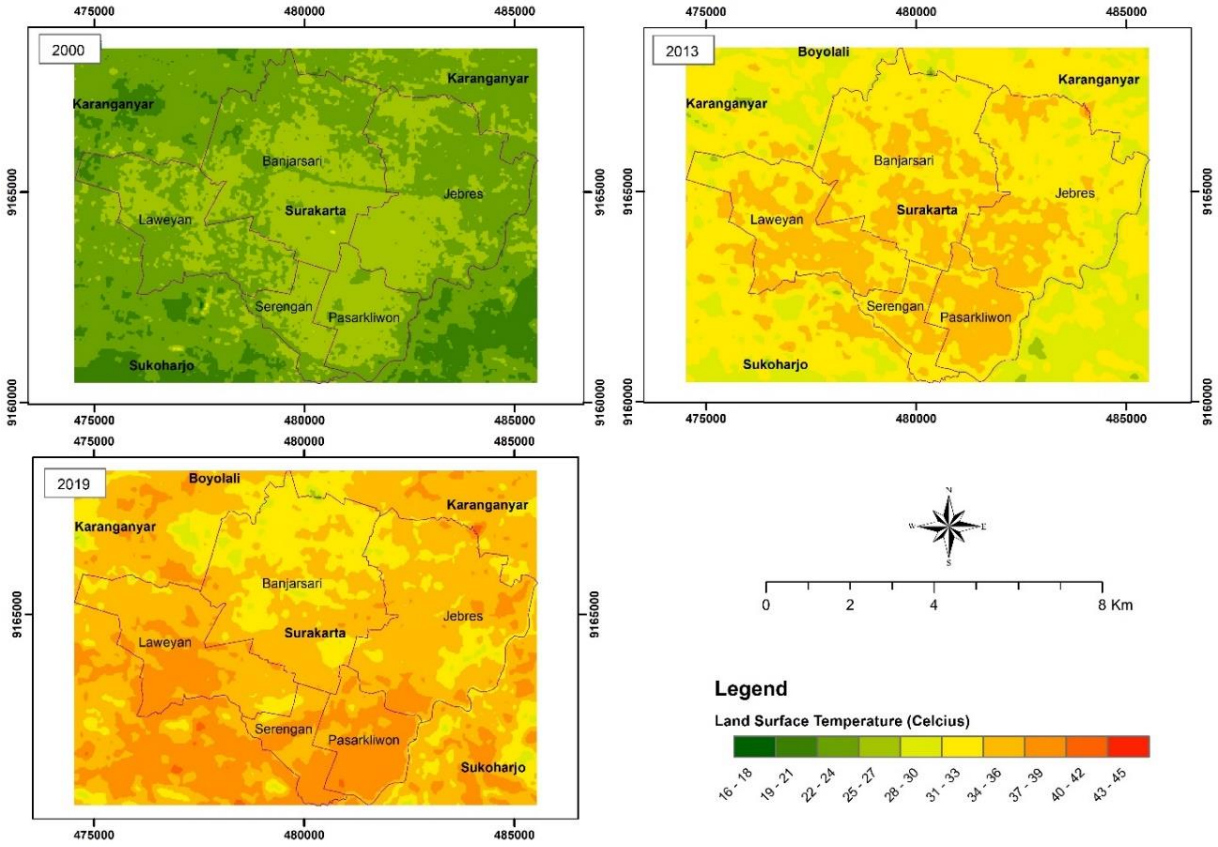

Figure 5. Distribution of land surface temperature in Surakarta and its surrounding areas.

Based on temperature observations in those three years, it is known that there has been an increase in surface temperature during the 19 years of observation, with the rising temperature

occurring more in the eastern and southern sides of the city of Surakarta, including its surroundings, such as Sukoharjo Regency. This condition is in line with the development of built-up areas measured by NDBI, where more built-up areas were seen on the eastern and southern sides of Surakarta City and its surrounding areas. In addition, this outcome is consistent with the major trend of population data shown in Table 1, since the southern part of Surakarta (Serengan and Pasar Kliwon) was a densely populated area. A previous study found that the continuously expanding population and housing demands accelerated the urbanization expansion, resulting in the substantial shift in built-up area shown from multitemporal NDBI (Hadeel et al., 2009). As a result, significant population growth could be regarded as one of the driving forces behind the transformation of the city's structure and morphology (Osgouei et al., 2019).

3.3. The relationship between built-up area and land surface temperature

The relationship between the distribution of built-up area and its land surface temperature was analyzed using a simple linear regression as shown in Figure 6. The result of correlation analysis with the R and R^2 values is presented in Table 4. For the year 2000, the regression equation was $y = 7.3363x + 23.881$ with $R = 0.737$ and a significance of $R^2 = 0.542$, but in 2013, the value of the equation was $y = 8.8828x + 32.199$, with $R = 0.680$ and the value of $R^2 = 0.463$. The regression equation for 2019 was $y = 9{,}394x + 34.409$, with $R = 0.439$ and $R^2 = 0.193$.

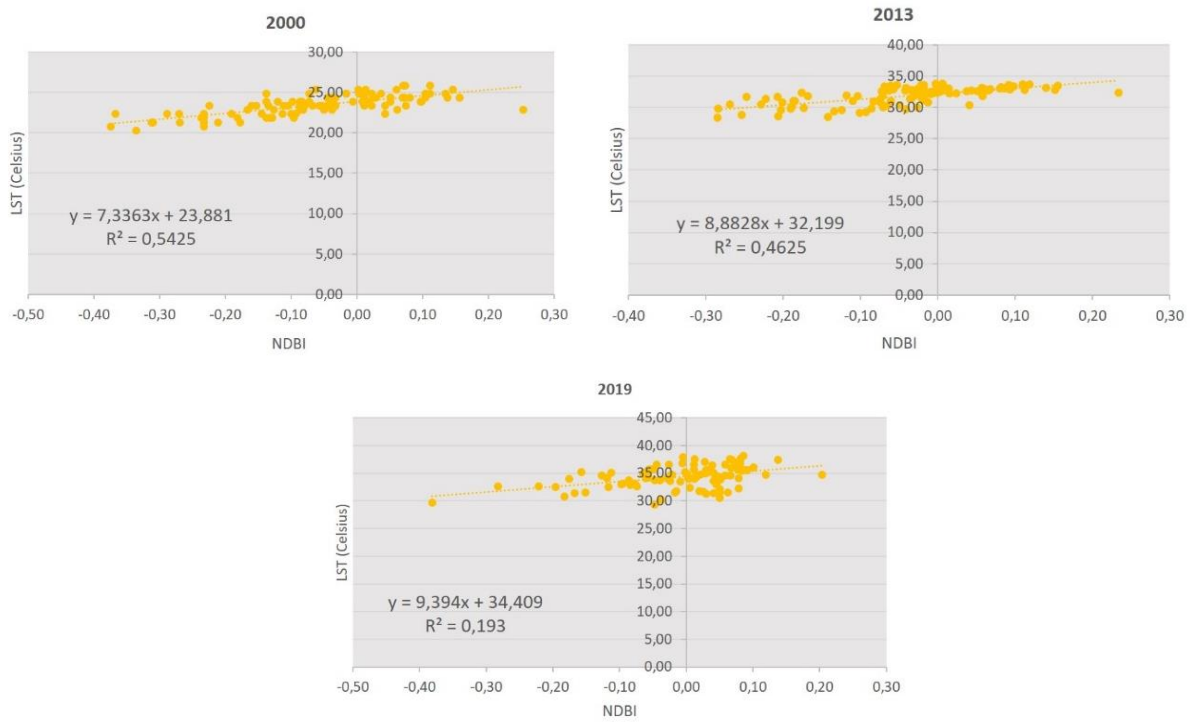

Figure 6. Regression between the NDBI and LST values for years 2000, 2013, and 2019.

Tabel 4. Value of R dan R^2 from a regression between NDBI and LST.

	Year		
	2000	2013	2019
R	0.737	0.680	0.439
R^2	0.542	0.463	0.193

Thus, all these equations produced positive values which indicate that the greater the NDBI index value, the higher the LST. The value of this equation also gave a quite high R (with an average

of 0.62), meaning that the NDBI value and surface temperature have a moderately strong correlation (Ratner, 2009). However, the resulting average R^2 value was quite low (below 50%). This suggests that there are other factors besides the built-up area that explain the changes in land surface temperature. Moreover, it was found that the R and R^2 in 2019 were the lowest among the observed periods. This indicates that other factors may have recently influenced the surface temperature. For instance, the urban morphology, which takes the height of buildings into consideration, also has an impact on surface temperature (Yin et al., 2022). For this reason, further study into the relationship of other factors to LST should be conducted, especially using additional remote sensing indices, such as the index of density and water content in vegetation and soil moisture.

4. Conclusion

The distribution of built-up area has been mapped in the city of Surakarta and its surroundings using the NDBI index processing. Based on the NDBI results, there was a rise in the distribution of built-up areas from 2000 to 2019, especially in the eastern and southern sides of Surakarta City, adjacent to Sukoharjo Regency. LST processing to obtain the surface temperature also showed an increase in temperature throughout the observation period. High temperatures could also be seen in the southern area of Surakarta City where the built-up area with high density is also located. Finally, the regression results revealed a positive linear relationship between the NDBI and LST values in all years of observation. However, the resulting low R^2 indicates that other factors besides the built-up area also affect LST which may be investigated in future research.

Acknowledgement

The authors would like to thank Universitas Muhammadiyah Surakarta (UMS) for supporting this study under the funding scheme of *'Penelitian Unggulan Program Studi'* at UMS.

References

Adeanti, M., & Harist, C. (2018). Analisis spasial kerapatan bangunan dan pengaruhnya terhadap suhu studi kasus di Kabupaten Bogor (Spatial Analysis of Building Density and Its Effect on Temperature). *Seminar Nasional Geomatika: Penggunaan dan Pengembangan Produk Inormasi Geospasial Mendukung Daya Saing Nasional*, *14*, 529–536.

Balew, A., & Korme, T. (2020). Monitoring land surface temperature in Bahir Dar city and its surrounding using Landsat images. *Egyptian Journal of Remote Sensing and Space Science*, *23*(3), 371–386. https://doi.org/10.1016/j.ejrs.2020.02.001

BPS. (2020). *Kota Surakarta dalam angka 2019*. BPS (Badan Pusat Statistik) Kota Surakarta.

Danardono, Sunariya, M. I. T., Fikriyah, V. N., & Cholil, M. (2021). Spatiotemporal variation of terrestrial carbon sequestration in tropical urban area (Case study in Surakarta District, Indonesia). *Quaestiones Geographicae*, *40*(3), 5–20. https://doi.org/10.2478/quageo-2021-0020

Deng, Z., Zhu, X., He, Q., & Tang, L. (2019). Land use/land cover classification using time series Landsat 8 images in a heavily urbanized area. *Advances in Space Research*, *63*(7), 2144–2154. https://doi.org/10.1016/j.asr.2018.12.005

Guha, S., Govil, H., Dey, A., & Gill, N. (2018). Analytical study of land surface temperature with NDVI and NDBI using Landsat 8 OLI and TIRS data in Florence and Naples city, Italy. *European Journal of Remote Sensing*, *51*(1), 667–678. https://doi.org/10.1080/22797254.2018.1474494

Hadeel, A. S., Jabbar, M. T., & Chen, X. (2009). Application of remote sensing and GIS to the study of land use/cover change and urbanization expansion in Basrah province, Southern Iraq. *Geo-Spatial Information Science*, *12*(2), 135–141. https://doi.org/10.1007/s11806-009-0244-7

Hadibasyir, H. Z., Rijal, S. S., & Sari, D. R. (2020). Comparison of land surface temperature during and before the emergence of Covid-19 using Modis Imagery in Wuhan City, China. *Forum Geografi*, *34*(1), 1–15. https://doi.org/10.23917/forgeo.v34i1.10862

Hidayati, I. N., Suharyadi, & Danoedoro, P. (2017). Pemetaan lahan terbangun perkotaan menggunakan pendekatan NDBI dan segmentasi semi-automatik. *Prosiding Seminar Nasional Geografi UMS 2017*, 19–28.

Hidayati, I. N., & Suharyadi, R. (2019). A comparative study of various indices for extraction urban impervious surface of Landsat 8 OLI. *Forum Geografi*, *33*(2), 162–172. https://doi.org/10.23917/forgeo.v33i2.9179

Imran, H. M., Hossain, A., Islam, A. K. M. S., Rahman, A., Bhuiyan, M. A. E., Paul, S., & Alam, A. (2021). Impact of land cover changes on land surface temperature and human thermal comfort in Dhaka City of Bangladesh. *Earth Systems and Environment*, *5*(3), 667–693. https://doi.org/10.1007/s41748-021-00243-4

Kabisch, N., Selsam, P., Kirsten, T., Lausch, A., & Bumberger, J. (2019). A multi-sensor and multi-temporal remote sensing approach to detect land cover change dynamics in heterogeneous urban landscapes. *Ecological Indicators*, *99*(July 2018), 273–282. https://doi.org/10.1016/j.ecolind.2018.12.033

Kalma, J. D., McVicar, T. R., & McCabe, M. F. (2008). Estimating land surface evaporation: A review of methods using remotely sensed surface temperature data. *Surveys in Geophysics*, *29*(4–5), 421–469. https://doi.org/https://doi.org/10.1007/s10712-008-9037-z

Kumari, B., Tayyab, M., Shahfahad, Salman, Mallick, J., Khan, M. F., & Rahman, A. (2018). Satellite-driven land surface temperature (LST) using Landsat 5, 7 (TM/ETM+ SLC) and Landsat 8 (OLI/TIRS) data and its association with built-up and green cover over urban Delhi, India. *Remote Sensing in Earth Systems Sciences*, *1*(3–4), 63–78. https://doi.org/10.1007/s41976-018-0004-2

Macarof, P., Bîrlica, I. C., & Stătescu, F. (2017). Investigating the relationship between land surface temperature and urban indices using landsat-8: a case study of Iaşi. *Lucrările Seminarului Geografic "Dimitrie Cantemir," 45*(0), 81–88. https://doi.org/10.15551/lsgdc.v45i0.07

Malik, M. S., Shukla, J. P., & Mishra, S. (2019). Relationship of LST, NDBI and NDVI using landsat-8 data in Kandaihimmat watershed, Hoshangabad, India. *Indian Journal of Geo-Marine Sciences*, *48*(1), 25–31.

Naserikia, M., Shamsabadi, E. A., Rafieian, M., & Filho, W. L. (2019). The urban heat island in an urban context: A case study of Mashhad, Iran. *International Journal of Environmental Research and Public Health*, *16*(3). https://doi.org/10.3390/ijerph16030313

Osgouei, P. E., Kaya, S., Sertel, E., & Alganci, U. (2019). Separating built-up areas from bare land in mediterranean cities using Sentinel-2A imagery. *Remote Sensing*, *11*(3), 1–24. https://doi.org/10.3390/rs11030345

Putri, P., & Zain, A. F. (2010). Analisis spasial dan temporal perubahan luas ruang terbuka hijau di kota Bandung. *Jurnal Lanskap Indonesia*, *2*(2), 115–121. https://doi.org/https://doi.org/10.29244/jli.2010.2.2.%p

Ratner, B. (2009). The correlation coefficient: Its values range between 1/1, or do they. *Journal of Targeting, Measurement and Analysis for Marketing*, *17*(2), 139–142. https://doi.org/10.1057/jt.2009.5

Rushayati, S. B., Shamila, A. D., & Prasetyo, L. B. (2018). The role of vegetation in controlling air temperature resulting from urban heat island. *Forum Geografi*, *32*(1), 1–11. https://doi.org/10.23917/forgeo.v32i1.5289

Srivanit, M., & Hokao, K. (2009). Thermal infrared remote sensing for urban climate and environmental studies: An Application for the City of Bangkok, Thailand. *ISPRS Journal of Photogrammetry and Remote Sensing*, *64*(4), 335–344. https://doi.org/10.1016/j.isprsjprs.2009.03.007

USGS EROS. (2018). USGS EROS Archive - Landsat Archives - Landsat 8 OLI (Operational Land Imager) and TIRS (Thermal Infrared Sensor) Level-1 Data Products. *Usgs*, *2014*.

Wiweka, W. (2014). Pola suhu permukaan dan udara menggunakan citra satelit Landsat Multitemporal. *Jurnal Ecolab*, *8*(1), 11–22. https://doi.org/10.20886/jklh.2014.8.1.11-22

Xiong, Y., Huang, S., Chen, F., Ye, H., Wang, C., & Zhu, C. (2012). The impacts of rapid urbanization on the thermal environment: A remote sensing study of Guangzhou, South China. *Remote Sensing*, *4*(7), 2033–2056. https://doi.org/10.3390/rs4072033

Yin, S., Liu, J., & Han, Z. (2022). Relationship between urban morphology and land surface temperature—A case study of Nanjing City. *PLoS ONE*, *17*(2 February), 1–17. https://doi.org/10.1371/journal.pone.0260205

Yuliastuti, N., Sudarto, J. P. H., & Semarang, S. H. T. (2012). Pengaruh perkembangan lahan terbangun terhadap kualitas lingkungan permukiman (Studi kasus: Kawasan pendidikan kelurahan tembalang). *Jurnal Presipitasi: Media komunikasi dan pengembangan teknik lingkungan*, *9*(1), 10–16.

Zhang, J., Wang, Y., & Li, Y. (2006). A C++ program for retrieving land surface temperature from the data of Landsat TM/ETM+ band6. *Computers and Geosciences*, *32*(10), 1796–1805. https://doi.org/10.1016/j.cageo.2006.05.001